U.S. DEPARTMENT OF ENERGY | Office of NUCLEAR ENERGY

Clean. Reliable. Nuclear.

Irradiation Behavior of Piezoelectric Materials for Nuclear Sensor Applications

Advanced Sensors & Instrumentation Annual Program Review

October 2022

Ryan Chesser - chesser.25@osu.edu
Prof. Marat Khafizov - khafizov.1@osu.edu

The Ohio State University

Introduction

- Ultrasonic sensors utilize sound wave propagation in a characteristic material.
- Wave propagation is sensitive to microstructural properties, and impacted by temperature, pressure, and stress/strain, introducing sensor applications.

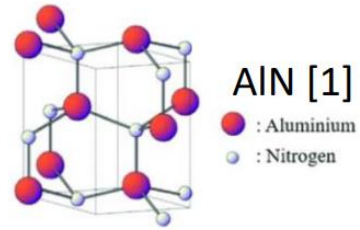

$LiNbO_3$ [2]

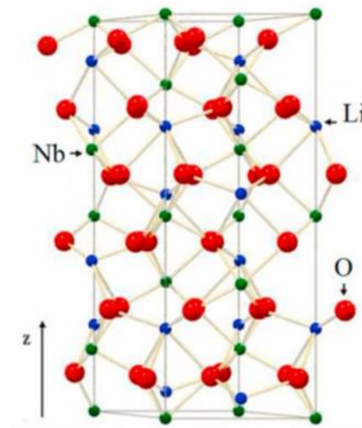

- In-pile instrumentation supports research with advanced fuels, models/simulations, and reactor designs.
- Opportunities are limited due to cost/risk.

[1] Alsaad, A.M., et. Al. (2020) Measurement and ab initio Investigation of Structural, Electronic, Optical, and Mechanical Properties of Sputtered Aluminum Nitride Thin Films, Front. Phys. 8:115.
[2] Anikiev, N.V., et. Al. (2021) Parametrization of Nonstoichiometric Lithium Niobate Crystals with Different States of Defectivity, Optical Materials, vol. 111

Surface Acoustic Waves (SAW)

- Piezoelectric materials convert input electrical signal to mechanical acoustic wave
- Wave velocity is sensitive to elastic constants, which are impacted by temperature and neutron flux [1]
- Characteristic SAW signal can be correlated to operating conditions

2.2 Numerical modelling

The Rayleigh SAW velocity can be analytically determined by solving elastic wave equations in an anisotropic media and taking into account piezoelectric effect [29]:

$$\rho \frac{\partial^2 u_i}{\partial t^2} = e_{kij} \frac{\partial^2 U}{\partial x_j \partial x_k} + C_{ijkl} \frac{\partial^2 u_k}{\partial x_j \partial x_l} \tag{2}$$

$$\varepsilon_{ij} \frac{\partial^2 U}{\partial x_j \partial x_i} - e_{ijk} \frac{\partial^2 u_j}{\partial x_i \partial x_k} = 0 \tag{3}$$

where $x_i, \rho, u_i, U, C, \varepsilon, e$, are spatial coordinate, density, displacement, electric potential, elastic tensor, dielectric tensor, and piezoelectric tensor, respectively. Material properties were

[1] Wang, et. Al., Nucl. Instrum. Meth. B., **481**, 35 (2020)

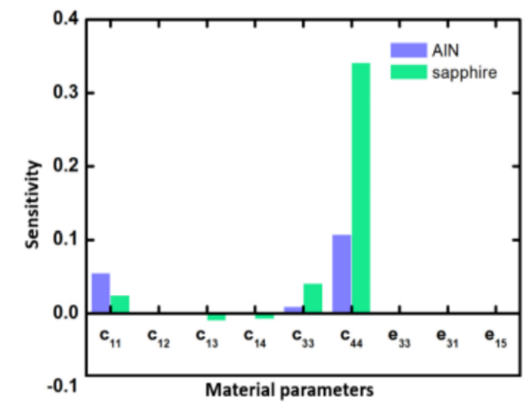

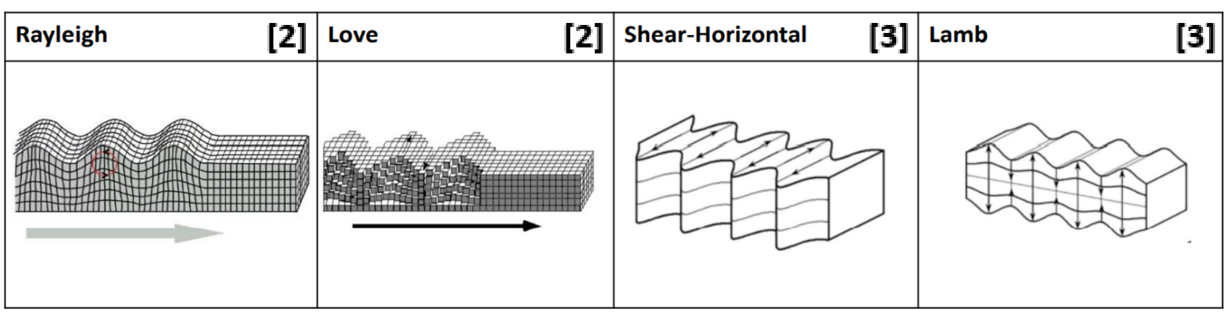

[3] *A. Muc et al. Composite Structures 255 (2021) 112930*

[2] (Modified from Bruce A. Bolt, *Earthquakes: A Primer.* W.H. Freeman & Company. 1978.)

SAW Applications

<u>SAW Applications</u>

- "Crystal oscillator" for telecommunications (such as quartz devices)
- Electrical components, actuators, RF filters
- Quantum Acoustics
- Fluid Flow
- **Sensors**

<u>SAW Sensors</u>

- Chemical, optical, thermal, pressure, acceleration, torque, biological
- Touchscreens
- Turbines
- Nuclear Reactors
- Space

Inherent
- Pressure
- Strain
- Torque
- Temperature
- Mass

Extended
- Chemical vapors
- Biological matter
- Humidity
- UV Radiation
- Magnetic Fields
- Viscosity

Experiment Design and Methods

- SAW sensor is fabricated via photolithography and platinum vapor deposition
- Coaxial cables are attached to sensors and extend to experiment equipment
- Sensor structure is loaded to Auxiliary Irradiation Facility (AIF) dry tube and positioned near reactor core
- Equipment Used:
  Keysight Network Analyzer

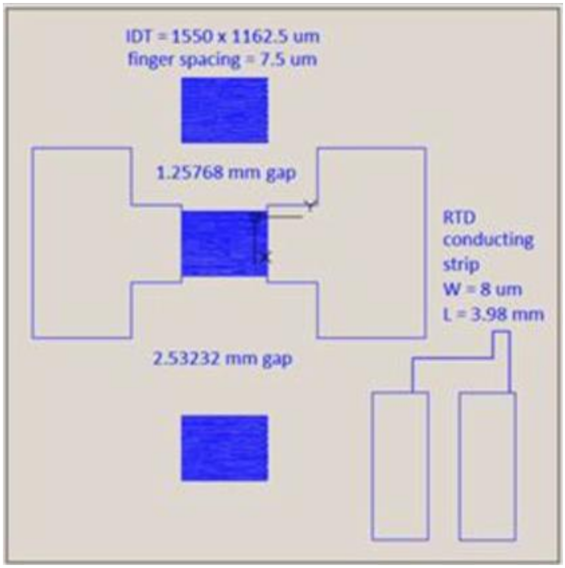

$$f_0 = \frac{v_{SAW}}{d}$$

f_0	Resonant frequency
v_{SAW}	Surface Acoustic Wave (SAW) velocity
d	Electrode periodicity (“pitch” or “gap length”)

$$\Gamma = S_{11} = \frac{\overline{Z_{in}} - Z_S}{\overline{Z_{in}} + Z_S} = \text{input port reflection coef.}$$

SAW Device Operation

- Employs Frequency Domain Reflectometry (FDR)
- SAW resonant frequency and amplitude change gradually, saturating with time

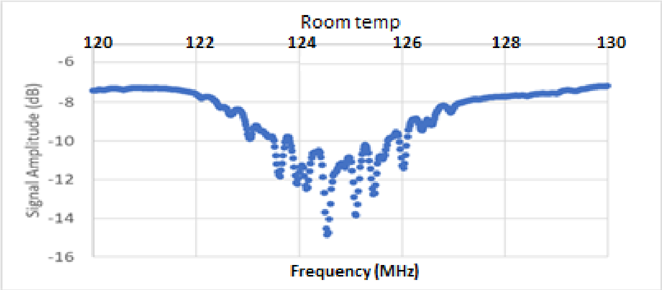

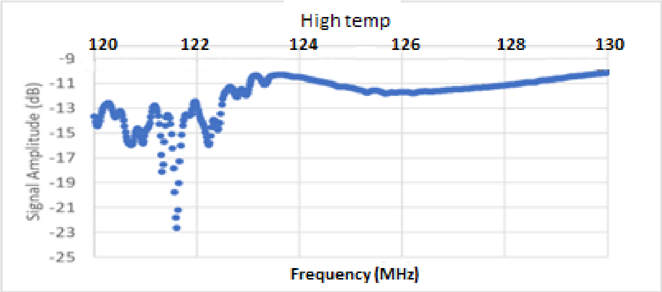

- Observed changes are attributed to neutron/gamma damage and gamma heating

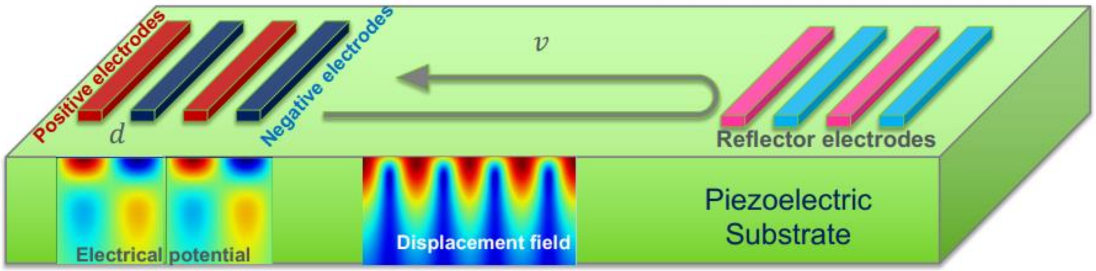

Experiment Results

Power steps:
$\lesssim$ 450 kW

Max total flux:
~1x10^{13} n/cm^{2}s

Max thermal flux:
~5x10^{12} n/cm^{2}s

Temperature:
$\lesssim$ 500°C

$\Delta f_{T,P} = \Delta f / f_0$

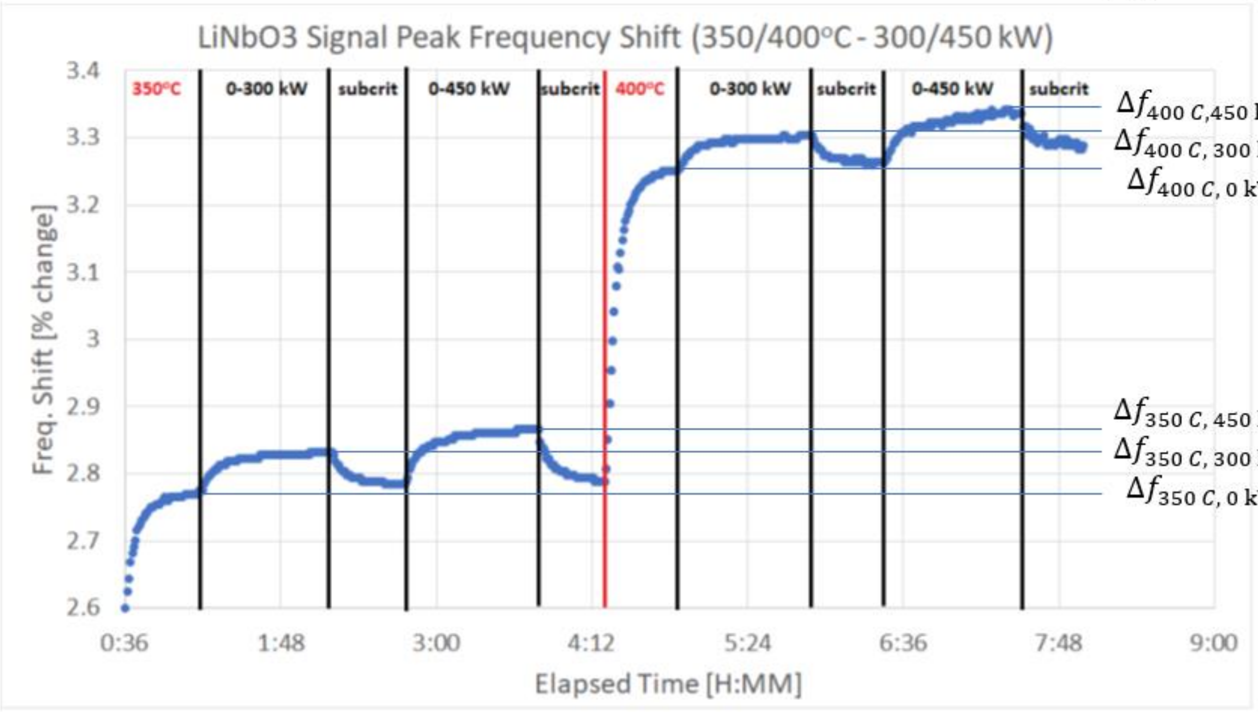

- **Goal:** Characterize temperature and reactor power effects <u>independently</u>

Note: $T \uparrow$ or $P \uparrow = f_{res} \downarrow$

Experiment Analysis – $LiNbO_3$

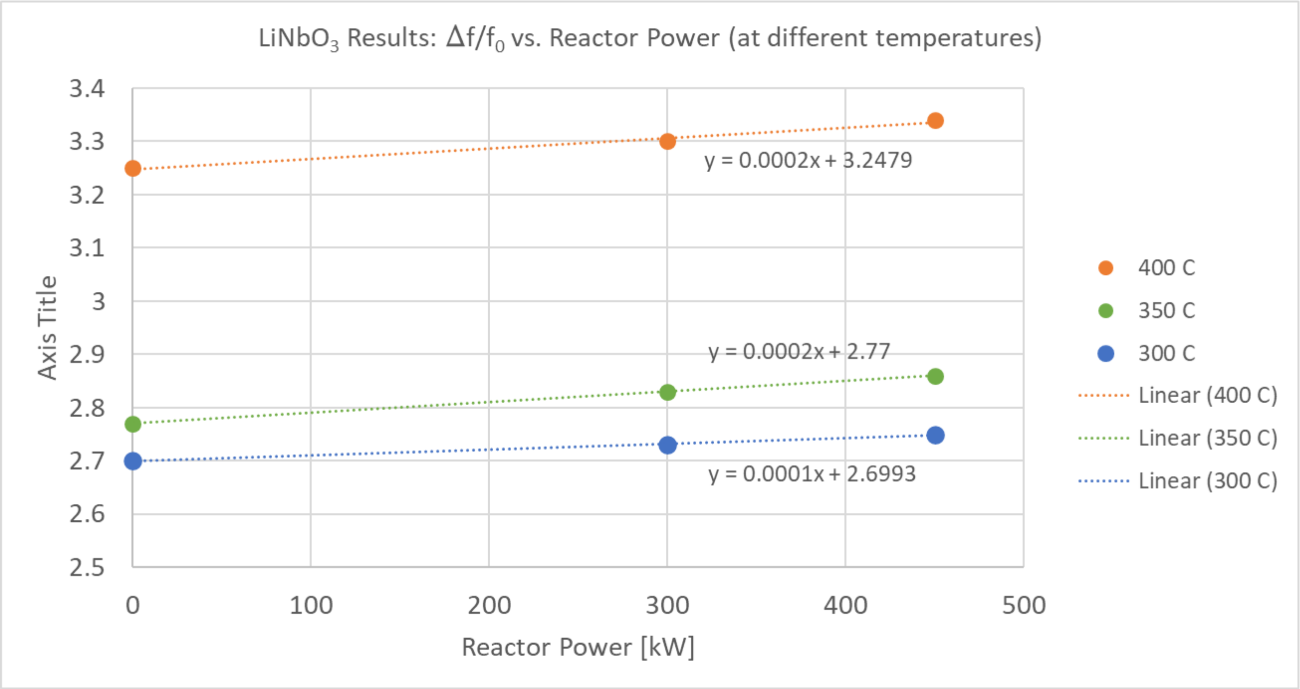

- Signals became unstable $> 400^{o}\mathrm{C}$
- Resonant frequency shifts linearly with reactor power
- Higher temperature causes larger response to power

Experiment Analysis – AlN

- Top:
  Single-crystal AlN
- Bottom:
  Thin-Film AlN on sapphire (AlN+)

- AlN+ has slightly larger response, likely due to sapphire (Al_2O_3) layer contribution

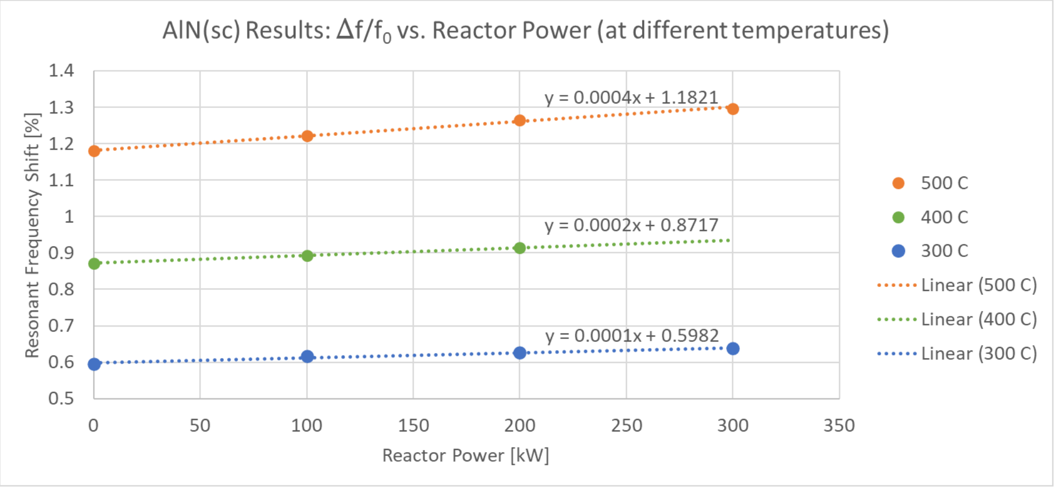

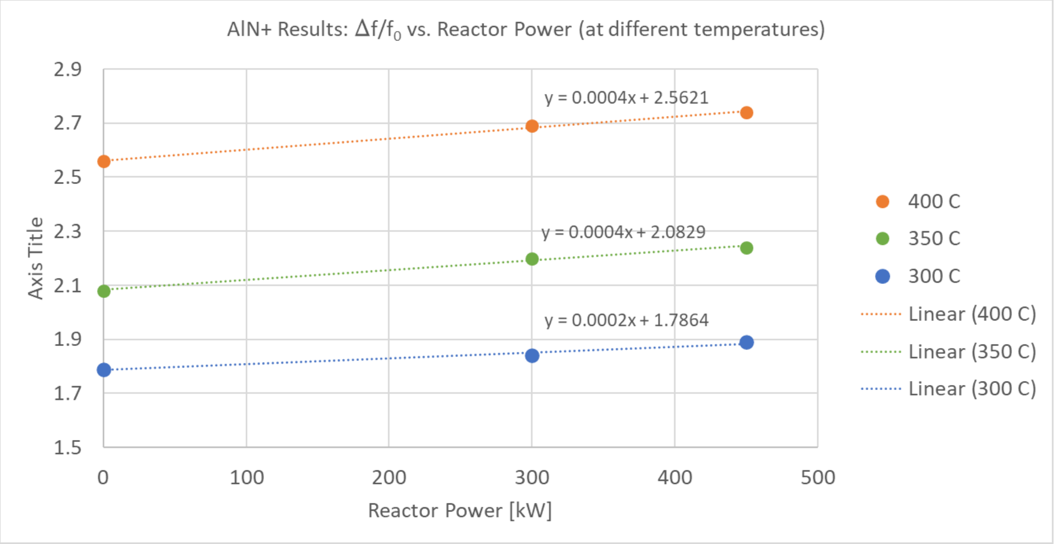

Concluding Remarks

Experiment Conclusions

- SAW sensors can monitor high temperature and reactor power
- Sensor response is dominated by shifting elastic constant
- Response kinetics offer clues about interaction mechanism(s)
- $LiNbO_3$ provides better signal/noise compared to AlN, but temperature is limited
- Signals are stable/repeatable

Acknowledgements

- This work was supported by the Advanced Sensors and Instrumentation (ASI) Program
- Services and materials provided by OSU Nanotech-West, Hexatech Inc., and MTI Corporation
- Special thanks to OSU Nuclear Reactor Lab and reactor staff members for irradiation services and tireless support
  - Joel Hatch, Kevin Herminghuysen, Andrew Kauffman, Maria McGraw, and Susan White
  - Website: reactor.osu.edu
    Email: reactor@osu.edu